Condensed Complexes of Cholesterol and Phospholipids

Arun Radhakrishnan and Harden M. McConnell
Department of Chemistry, Stanford University, Stanford, California 94305 USA

ABSTRACT Mixtures of dihydrocholesterol and phospholipids form immiscible liquids in monolayer membranes at the air-water interface under specified conditions of temperature and 2-dimensional pressure. In recent work it has been discovered that a number of these mixtures exhibit *two* upper miscibility critical points. Pairs of upper critical points can be accounted for by a theoretical model that implies the cooperative formation of molecular complexes of dihydrocholesterol and phospholipid molecules. These complexes are calculated to be present in the membranes both above and below the critical points. Below the critical points the complexes form a separate phase, whereas above the critical points the complexes are completely miscible with the other lipid components. The cooperativity of complex formation prompts the use of the terminology *condensed complex.*

INTRODUCTION

There have been numerous physical chemical studies of mixtures of cholesterol and phospholipids in monolayer as well as bilayer membranes (Feingold, 1993). Aside from their biological relevance, these mixtures have been of interest because they show strongly nonideal mixing behavior. This behavior has variously been interpreted in terms of a "condensing effect" of cholesterol, the formation of specific cholesterol-phospholipid complexes, phase separation into co-existing liquid phases, or the formation of superlattices. Despite this extensive earlier experimental and theoretical work, there is need for a single, inclusive, quantitative model for the various properties of these mixtures. The work presented here arose from an unanticipated discovery of pairs of upper liquid-liquid miscibility critical points in mixtures of dihydrocholesterol (DChol) and phospholipids at the air-water interface (Radhakrishnan and McConnell, 1999). In interpreting these results we were led to a model in which molecular complexes of DChol and phospholipids are formed. There is an associated reduction in molecular area, commonly referred to as a "condensation." Under special conditions this process leads to two upper miscibility critical points. A novel feature of the present model is the molecular cooperativity involved in complex formation. The model is general enough to incorporate the idea of a superlattice structure. It predicts sharp features in the average area per molecule at the complex stoichiometries, a prediction that is verified experimentally.

The thermodynamic model relies heavily on two theoretical papers, one by Corrales and Wheeler (1989) and the other by Talanquer (1992). These authors have calculated phase diagrams for two-component liquid mixtures in which the components undergo a reversible chemical reaction to form a third liquid component. We have elaborated their mean field thermodynamic model to include a pressure dependence of the free energy and the formation of oligomeric complexes. There have been a number of earlier theoretical treatments of cholesterol-phospholipid mixtures. These treatments have considered various aspects of the problem of liquid-liquid immiscibility as well as complex formation (Ipsen et al., 1987; Slater and Caille, 1981). None of the earlier work has considered multiple upper miscibility critical points, which has been the motivation for the present study.

A preliminary report of this work is given elsewhere (Radhakrishnan and McConnell, 1999). That report is one of a series of studies of liquid-liquid immiscibility in DChol-phospholipid mixtures in monolayers at the air-water interface (Hagen and McConnell, 1996, 1997). DChol, rather than cholesterol, has often been used to minimize air oxidation (Benvegnu and McConnell, 1993). These studies rely on the use of epifluorescence microscopy to observe co-existing liquid phases. There are two special aspects to this experimental work. In certain cases the lipid domains formed are so small they are difficult to resolve in the optical microscope. These small domains can be fused with one another through the use of an externally applied electric field (Lee et al., 1994). The field is then removed before subsequent measurements. The second point concerns the identification of critical points in the phase diagrams. Near critical points the monolayer domains form stripes, and the observation of these stripes is very useful for the determination of the critical compositions and pressures (Keller and McConnell, 1999). Both experimental techniques have been important in the identification of pairs of upper miscibility critical points.

We assume that properties of lipid monolayers are closely similar to those of bilayers under appropriate conditions of temperature and pressure. Accordingly, we anticipate that this work may be useful in connection with recent studies of biological membranes involving the "liquid ordered phase" (Feingold, 1993), or the "detergent resistant phase" (Brown and Rose, 1992; Brown and London, 1998; Sheets et al., 1999; Cinek and Horejsi, 1992; Bohuslav et al., 1993;

Received for publication 8 March 1999 and in final form 21 May 1999.
Address reprint requests to Dr. Harden McConnell, Dept. of Chemistry, Stanford University, Stanford, CA 94305-5080. Tel.: 650-723-4571; Fax: 650-723-4943; E-mail: harden@leland.stanford.edu.

0006-3495/99/09/1507/11 $2.00

Hanada et al., 1995). Our calculations also appear relevant to the work of Brown and Goldstein (1999) on the regulation of cholesterol biosynthesis.

EXPERIMENTAL

The experimental phase diagrams in Fig. 2, *a–c* were obtained for mixtures of DChol and phospholipids using epifluorescence microscopy and methods described previously (Subramaniam and McConnell, 1987; Hirshfeld and Seul, 1990). In Fig. 2 *a,* the phospholipid is a 2:1 molar mixture of dimyristoylphosphatidylserine (DMPS) and dimyristoyl-phosphatidylcholine (DMPC). A small amount (0.2 mol %) of a fluorescent dye, Texas red dimyristoylphosphatidyl-ethanolamine (TR-DMPE), which is preferentially excluded from the DChol-rich phase, is used to provide contrast between phases. Lipids were deposited from 1 mg/mL chloroform solutions on the air-water interface of a 9 cm × 2.5 cm Teflon trough that had a movable barrier to modulate the surface pressure. The subphase contained distilled water at pH 5.3; substitution of phosphate-buffered saline at pH 7.0 made no significant difference. The domains formed in the α two-phase coexistence region of Fig. 2 *a* were circular (5–10 μm) and easily resolved microscopically, as shown in Fig. 1 *a.* However, the domains formed in the β two-phase coexistence region were typically very small (Fig. 1. *c*). An electric field was used to fuse some of the domains, thereby making them easier to observe. This method has been described in detail in earlier work (Lee et al., 1994). The electric field was turned off before making subsequent measurements of the phase transition pressures. The critical points can be identified by the observation of the superstructure stripe phase, which is only seen close to the critical pressure and composition (Keller and McConnell, 1999). Epifluorescence micrographs of the stripe phase in both the α and β regions are shown in Fig. 1, *b* and *d.* The experiments do not preclude the possible existence of more than two upper critical points. Fig. 2, *b* and *c* show phase diagrams derived in a similar fashion for other lipid mixtures of DChol and phospholipids. In Fig. 2 *b,* the phospholipid is DMPS only, while in Fig. 2 *c,* the phospholipid is a 1:1 molar mixture of DMPC and dipalmitoyl-phosphatidylcholine (DPPC). The binary system of DChol and DMPS in Fig. 2 *b* shows that the observation of two upper critical points is not dependent on the use of a ternary lipid mixture rather than a binary mixture. All of the above lipids, DMPC, DPPC, DMPS (Avanti Polar Lipids, Alabaster, AL), DChol

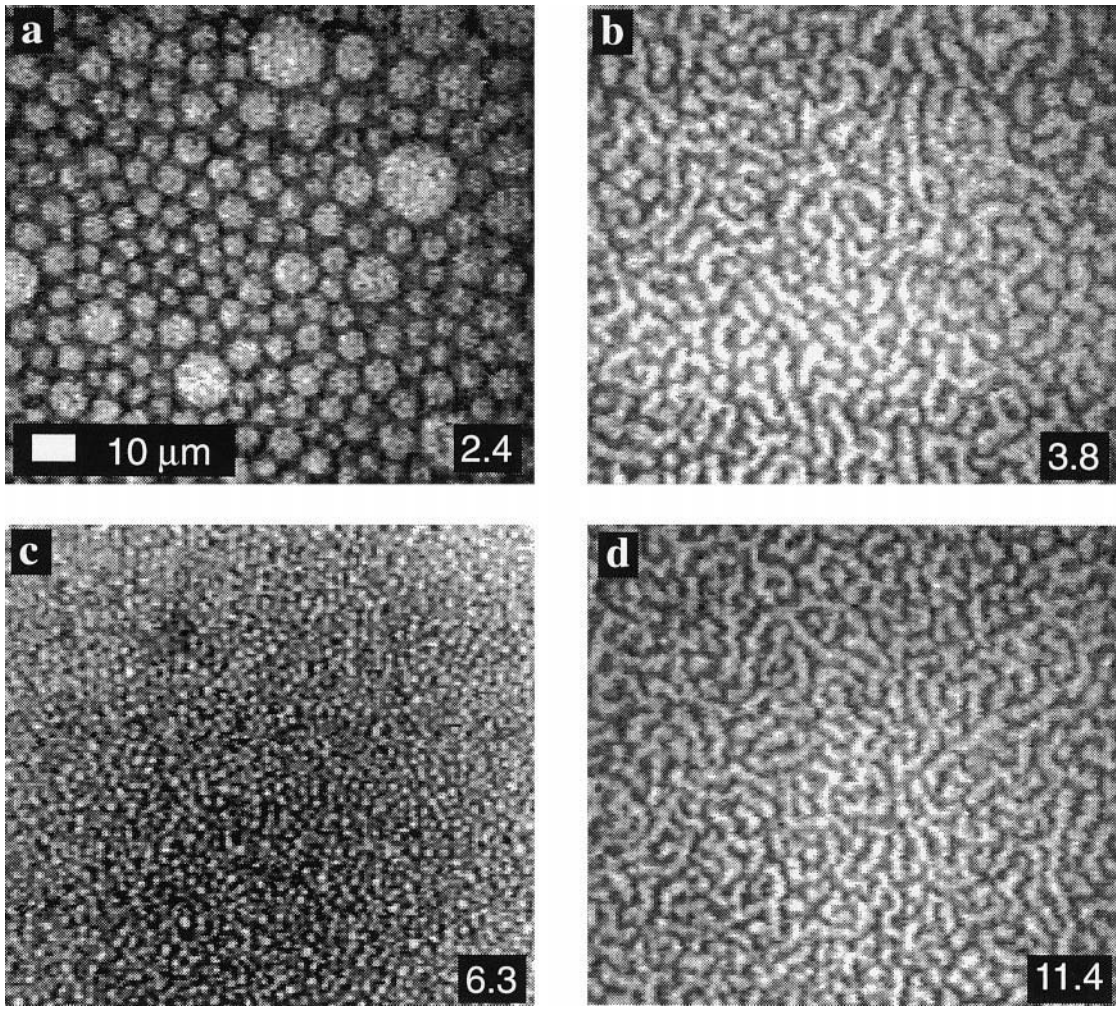

FIGURE 1 Epifluorescence micrographs of a lipid monolayer consisting of DMPC, DMPS, and DChol at various pressures at an air-water interface at room temperature (23°C). (*a*) and (*b*) show images of a monolayer consisting of 25 mol % DChol, 49.9 mol % DMPS, 24.9 mol % DMPC, and 0.2 mol % TR-DMPE. (*a*) 2.4 mN/m: 5–10-μm circular domains of bright, DChol-poor liquid phase within a dark, DChol-rich liquid phase. These domains exhibit Brownian motion and are characteristic of domains formed in the α two-phase coexistence region of Fig. 2, *a–c.* (*b*) 3.8 mN/m: stripe phase characteristic of proximity to a miscibility critical point. (*c*) and (*d*) show images of a monolayer consisting of 50 mol % DChol, 32.2 mol % DMPS, 16.6 mol % DMPC, and 0.2 mol % TR-DMPE. (*c*) 6.3 mN/m. These small white domains are <2 μm in diameter and are formed in the β two-phase coexistence region of Fig. 2, *a–c.* (*d*) 11.4 mN/m. This stripe phase is characteristic of proximity to a miscibility critical point.

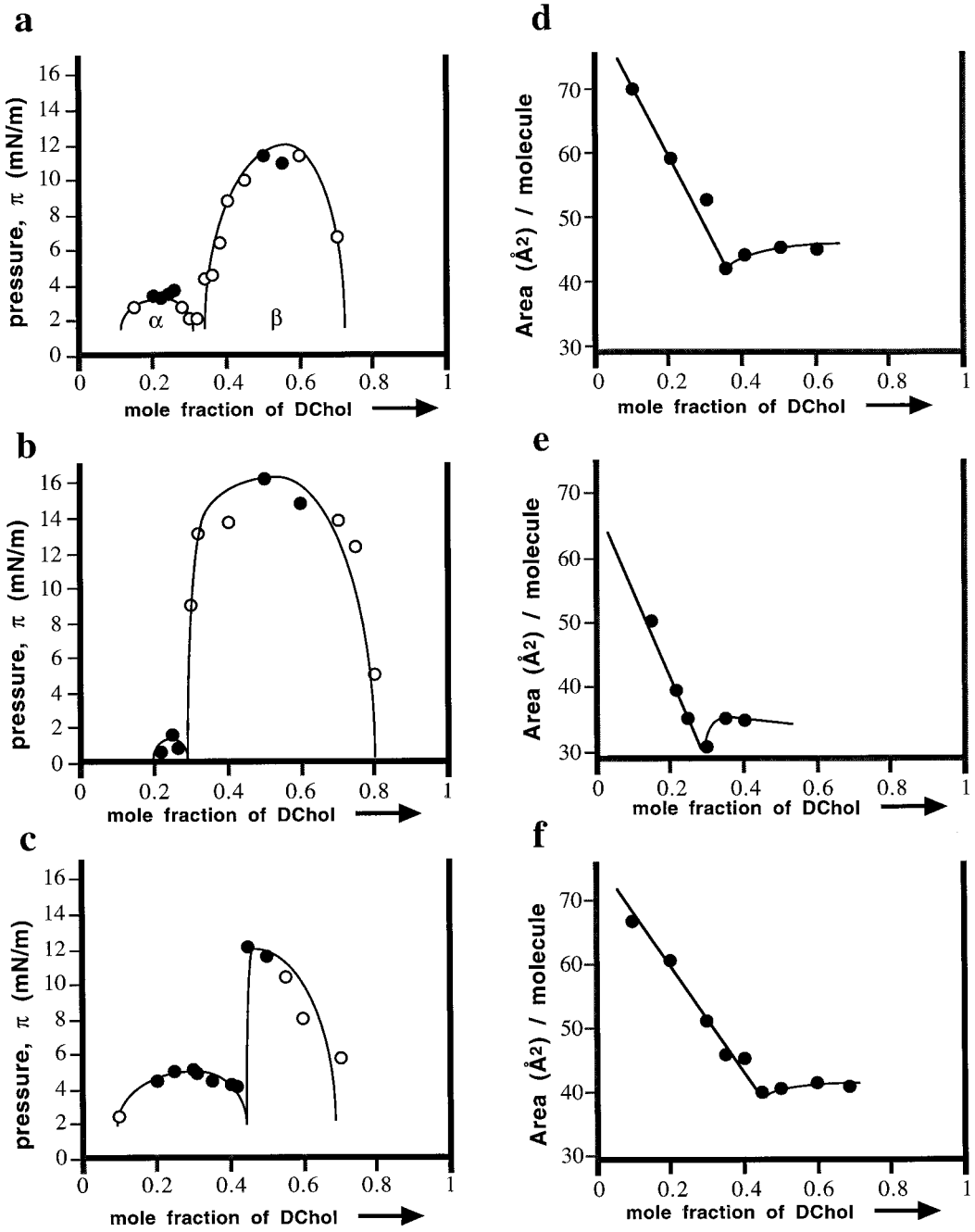

FIGURE 2 Phase diagrams showing liquid-liquid miscibility critical points and average molecular area measurements. (*a–c*) Phase diagrams for mixtures of DChol (mole fraction x_0) and phospholipids (mole fraction $1 - x_0$). (*a*) The phospholipid is a 2:1 molar mixture of DMPS and DMPC. (*b*) The phospholipid is DMPS only. (*c*) The phospholipid is a 1:1 molar mixture of DMPC and DPPC. In (*a–c*) the plotted data points represent the transition pressures that mark the disappearance of two-phase coexistence during monolayer compression, and thus define a phase boundary between a two-phase coexistence region at low pressures and a one-phase region at higher pressures. Stripe superstructure phases, which represent a proximity to a critical point, were observed at the transitions marked by filled circles, and not at those marked by the open circles. The two-phase coexistence region corresponding to low DChol mole fraction is referred to as α, and the two-phase coexistence region corresponding to high DChol mole fraction is referred to as β. (*d*) Average molecular area for the lipid mixture of (*a*) at a pressure of 3 mN/m. (*e*) Average molecular area for the lipid mixture of (*b*) at a pressure of 25 mN/m. (*f*) Average molecular area for the lipid mixture of (*c*) at a pressure of 3 mN/m. Typical errors for the above measurements are 3–8%.

(Sigma, St. Louis, MO), and TR-DMPE (Molecular Probes, Eugene, OR) were used without further purification.

Fig. 2, *d–f* show molecular area measurements for the lipid mixtures corresponding to Fig. 2, *a–c.* Aliquots of lipids were added until a specified surface pressure was reached and the corresponding area per molecule was then calculated. Fig. 2, *d* and *f* show molecular area measurements at a pressure of 3 dynes/cm, whereas Fig. 2 *e* shows a molecular area measurement for a pressure of 25 dynes/cm. These plots show sharp features at the same compositions as the cusps in the phase diagrams both above and below the critical pressures.

THEORETICAL MODEL

Theoretical work by Corrales and Wheeler (1989), and by Talanquer (1992), considers a reversible chemical reaction between the binary components of a liquid mixture to produce a third liquid component. Accordingly, we consider a "chemical reaction" between cholesterol (C) and phospholipids (P) to form a complex,

$$qC + pP \leftrightarrow C_qP_p \tag{1}$$

For later convenience q and p are taken to be relatively prime integers. The standard free energy change $\Delta G^0 = -kT \ln K_0$ and the equilibrium constant K_0 are related to the standard chemical potentials μ^0_C, μ^0_P, and $\mu^0_{C_qP_p}$ by the equation

$$\Delta G^0 = \mu^0_{C_qP_p} - q\mu^0_C - p\mu^0_P \tag{2}$$

A regular solution model for the free energy of this mixture is

$$\begin{aligned} G &= NkT(x \ln x + y \ln y + z \ln z) \\ &\quad + NkT_r(ayz + bxz + cxy) + N(x\mu^0_C + y\mu^0_P + z\mu^0_{C_qP_p}) \end{aligned} \tag{3}$$

Here x, y, and z are the mole fractions of cholesterol (or DChol), phospholipid, and complex (C_qP_p), respectively, and a, b, and c are energy parameters representing a mean field "repulsion" between the several molecular pairs. N is the equilibrium number of molecules in the sample. To simplify the notation, in the following the letters x, y, z in the subscripts stand for cholesterol, phospholipid, and complex, respectively. Since we are concerned with experiments carried out at room temperature, the repulsion energies are given in units of a room temperature energy, kT_r. These parameters depend linearly on the pressure,

$$\begin{aligned} a &= 2 + a'(\pi - \pi_{yz}) \\ b &= 2 + b'(\pi - \pi_{xz}) \\ c &= 2 + c'(\pi - \pi_{xy}) \end{aligned} \tag{4}$$

Here π_{xy}, π_{yz}, and π_{xz} are the critical pressures of hypothetical nonreacting binary mixtures of cholesterol and phospholipids, phospholipids and complex, and cholesterol and complex, respectively. The terms in Eq. 4 give rise to a pressure dependence of the free energy G in Eq. 3.

Previous work related a parameter similar to c' to the experimentally observed nonideality of mixing of mixtures of cholesterol and phospholipids (Hagen and McConnell, 1996; Lee et al., 1994). That is, when the molecular area A_{xy} of a mixture of cholesterol and phospholipids is assumed to deviate from ideality according to the equation

$$A_{xy} = xA^0_x + yA^0_y + 2\Delta_{xy}xy \tag{5}$$

it follows that

$$c' = \Delta_{xy} \tag{6}$$

In subsequent numerical calculations a', b' and c' have been limited to be of the order of magnitude of observed deviations from area additivity.

A pressure dependence of the free energy G also arises from the pressure dependence of the chemical potentials and the dependence of the equilibrium constant on these chemical potentials. For example,

$$\mu^0_x(\pi) = \mu^0_x(\pi_0) + A^0_x(\pi - \pi_0) \tag{7}$$

In the calculations the free energy G is minimized with respect to the reaction progress parameter γ, defined in the equation,

$$\gamma = (N_z)/[N_x + N_y + (p + q)N_z]. \tag{8}$$

Here, N_x, N_y, and N_z are the equilibrium number of molecules of cholesterol, phospholipid, and complex. The mole fractions of the three components can be expressed in terms of this reaction progress variable and the initial mole fractions of cholesterol and phospholipid:

$$\begin{aligned} z &= \gamma\zeta \\ y &= (y_0 - p\gamma)\zeta \\ x &= (x_0 - q\gamma)\zeta \\ \zeta &= [1 + (1 - p - q)\gamma]^{-1} \end{aligned} \tag{9}$$

Here, x_0 and y_0 are the mole fractions of cholesterol and phospholipid in the sample before reaction. The above equations can be combined to obtain the following expression for the free energy,

$$\begin{aligned} \frac{G}{N^0kT_r} &= t[(x_0 - q\gamma) \ln((x_0 - q\gamma)\zeta) + (y_0 - p\gamma) \ln((y_0 \\ &\quad - p\gamma)\zeta) + \gamma \ln(\gamma\zeta)] \\ &\quad + \zeta[a(y_0 - p\gamma)\gamma + b(x_0 - q\gamma)\gamma \\ &\quad + c(x_0 - q\gamma)(y_0 - p\gamma)] \\ &\quad - \gamma t \ln K_0 + \gamma\Delta A\pi/kT_r \end{aligned} \tag{10}$$

In writing this equation we have set the reference pressure equal to zero, $\pi_0 = 0$, let K_0 represent the equilibrium constant at zero pressure, $t = T/T_r$, $N^0 = N_x + N_y + (p + q)N_z$, and set the area change on reaction equal to $\Delta A = A^0_z - qA^0_x - pA^0_y$. In addition, terms are dropped that do not depend on γ, such as $x_0\mu^0_x(\pi_0) + y_0\mu^0_y(\pi_0)$ and $(x_0A^0_x + y_0A^0_y)(\pi - \pi_0)$. These terms are also omitted in the subsequent calculations of the free energy and phase diagrams, as they do not have any qualitatively significant effects.

From Eq. 10 it will be seen that the free energy can be expressed as a function of three variables, $G = G(x_0, \pi, \gamma)$, along with a number of parameters. The calculated phase diagrams were constructed from this free energy function by first minimizing G with respect to γ for given values of composition x_0 and pressure π. The values of γ so obtained,

γ_{min}, then yield a free energy function $G(x_0, \pi, \gamma_{min})$ from which the phase diagrams are determined by the method of double tangent construction. Fig. 3 shows typical free energy functions $G(x_0, \pi, \gamma_{min})$ used in the construction of the phase diagrams. Fig. 3 *a* gives rise to two two-phase coexistence regions for lipid compositions between the two sets of tangent points, while Fig. 3, *b* and *c* give rise to a single two- and three-phase coexistence region, respectively. In some cases (not shown) the plots of $G(x_0, \pi, \gamma)$ show two minima as a function of γ. A switch in the relative depth of the two minima gives rise to a first-order phase transition in which the degree of complex formation changes discontinuously. When the discontinuous change in degree of complex formation occurs at a single point in the phase diagram without phase separation, this composition point is called an *areatrope* (Corrales and Wheeler, 1989).

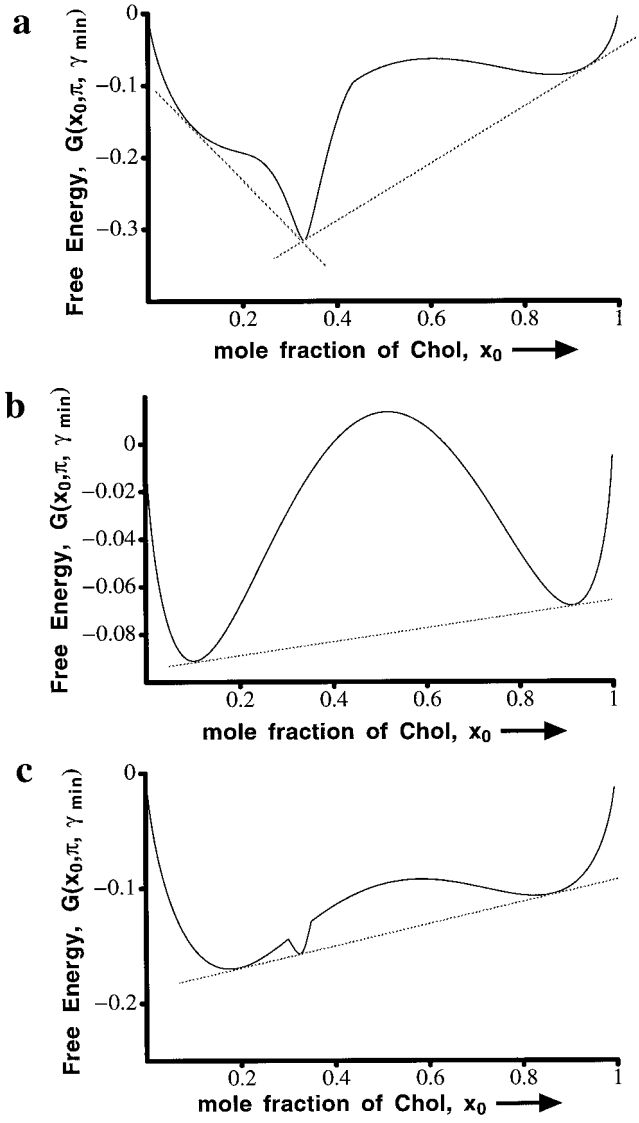

FIGURE 3 Calculated free-energy profiles as a function of the initial mole fraction of cholesterol (Chol), x_0, using Eq. 10. The parameters used in (*a–c*) are $t = 1$, $p = 2$, $q = 1$, $a' = -0.33$ m/mN, $b' = -0.5$ m/mN, $c' = -0.33$ *m/mN*, $\pi_{xy} = 3.3$ mN/m, $\pi_{xz} = 6$ mN/m, $\pi_{yz} = 3.3$ mN/m, and $\Delta A = -40$ Å^2. (*a*) $\pi = 0.2$ mN/m, and $K_0 = 2$. Lipid compositions between the two sets of tangent points exhibit two-phase coexistence. (*b*) $\pi = 0.2$ mN/m and $K_0 = 0.5$. In this case, there is only one two-phase coexistence region. (*c*) $\pi = 1.07$ mN/m, and $K_0 = 0.5$. In this case, the tangent line construction reveals a three-phase coexistence region.

Illustrative calculated phase diagrams, where the phase boundaries are determined using the method of double tangent construction, are given in Fig. 4. Fig. 4 *a* gives a phase diagram corresponding to the case where there is no complex formation, $K_0 = 0$, and where the critical pressure is $\pi_{xy} = 3.3$ dynes/cm. Two phase boundaries are given, illustrating how the value of c' affects the shape of these curves. The value of c' also determines the rate of change of the critical temperature with pressure, $\partial T_c/\partial \pi = 1/2(T_t c')$. Fig. 4, *b* and *c* illustrate the effect of complex formation on these diagrams for various values of the parameters. The critical pressures π_{xz}, π_{yz} have been set equal to typically observed critical pressures. The phase diagrams are relatively insensitive to changes in the invisible critical pressure π_{xy} when this pressure is in the range 2–5 dynes/cm. The values of a', b' affect the shape of the curves with two upper miscibility critical points in much the same way as c' affects the curve with one upper miscibility critical point in Fig. 4 *a.* It will be seen that as the equilibrium constant for complex formation is varied from small ($K_0 = 0$) in Fig. 4 *a* to large ($K_0 = 2$) in Fig. 4 *c,* there is a systematic change in the depth of the cusp. For an intermediate equilibrium constant ($K_0 = 0.5$) the complex is stable above a certain pressure (1.07 mN/m) and less stable below that pressure. This condition of three phase coexistence is illustrated in the free energy curve in Fig. 3 *c.*

Fig. 5 shows plots of the mole fraction of complex, *z*, as a function of pressure and composition. It will be seen that even at pressures above the critical pressures there is a strongly cooperative dependence of the degree of complex formation on sample composition. The sharp dependence of *z* on composition led us to expect relatively sharp features in area versus composition plots, even at pressures above the critical pressures. Plots of areas made with calculated compositions and assumed molecular areas are shown in Fig. 6 for various pressures both above and below the critical pressures. The molecular area experiments in Fig. 2, which were carried out as a test of the model, yielded curves with sharp features at the cusp compositions as predicted.

DISCUSSION

The present study has shown that a thermodynamic model describing a cooperative "chemical reaction" between cholesterol and phospholipids accounts for the observation of two upper miscibility critical points in some mixtures of these lipids in monolayers at the air-water interface. No effort has been made to obtain a precise fit of the observed phase diagrams with the model parameters. We are most concerned with the physical significance of the model, its possible generalization, and the breadth of its applicability to phospholipid-cholesterol mixtures.

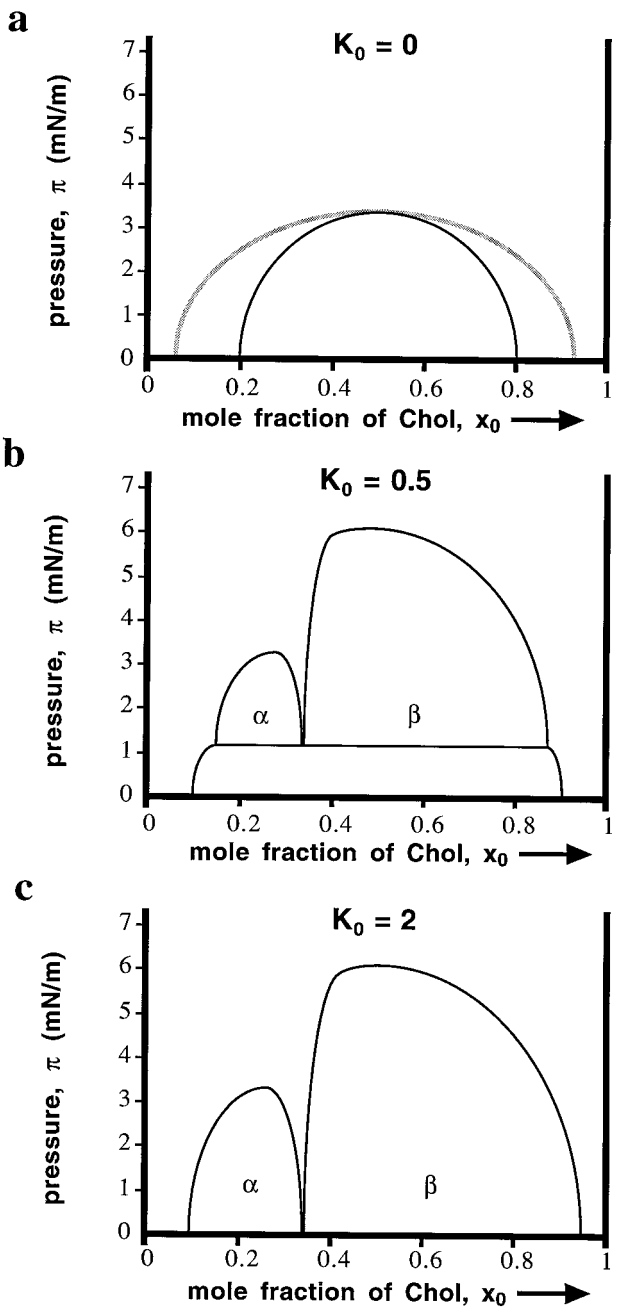

FIGURE 4 Calculated phase diagrams as a function of the initial mole fraction of cholesterol (Chol), x_0, for a binary reactive mixture of Chol and phospholipids for different values of the equilibrium constant K_0. The calculations in (*a–c*) use values of $t = 1, p = 2, q = 1, a' = -0.33$ m/mN, $b' = -0.5$ m/mN, $c' = -0.33$ m/mN, $\pi_{xy} = 3.3$ mN/m, $\pi_{xz} = 6$ mN/m, $\pi_{yz} = 3.3$ mN/m, and $\Delta A = -40$ Å^2. (*a*) No reaction, $K_0 = 0$. The effect of c' on the shape of the phase diagram is shown. The gray line depicts the phase diagram when $c' = -0.33$ m/mN, and the black line depicts the phase diagram when $c' = -1$ m/mN. (*b*) $K_0 = 0.5$. (*c*) $K_0 = 2$.

One of the important results is the finding that the calculated concentration of the complex is strongly peaked, even in the homogeneous phase, as illustrated in Fig. 5. This complex concentration versus composition profile is to be contrasted with that expected for an ideal reaction, illustrated in Fig. 7 *a*. By way of comparison, Fig. 7 *b* shows the calculated complex concentration versus composition profile appropriate to an oligomerization reaction,

$$nqC + npP \leftrightarrow C_{nq}P_{np} \tag{11}$$

The apparent cooperativity of the complex formation reaction in Fig. 5 *a* is comparable to that of an oligomerization with $n \approx 10$.

The theoretical results in Fig. 5 led us to carry out the molecular area measurements shown on the right-hand side of Fig. 2. These measurements show sharp features at the same compositions as the cusps in the phase diagrams. As far as we know these sharp features in molecular area versus composition plots have not been reported previously. The calculated areas also show sharp features at these compositions. These results are reassuring with respect to the validity of the model, particularly the evidence for cooperative complex formation, even above the critical pressures.

The cooperative complex formation shown in Fig. 5 is driven by the repulsion terms (immiscibility parameters) in Eq. 3. The complexes are obviously physically close to one another when present as a separate phase. The model says nothing about the physical proximity of the complexes above the critical points in the homogeneous phase at various membrane compositions, but one would expect an improved model to show an enhanced proximity. To emphasize the point that the complex is not simply an isolated group of $p + q$ molecules, but is rather a group of molecules strongly affected by the (mean-field) environment, we express the reaction of complex formation as follows,

$$qC + pP \leftrightarrow \langle C_qP_p \rangle \tag{12}$$

The symbol $\langle C_qP_p \rangle$ is thus used to represent the *condensed complex.*

This putative physical proximity of complexes can be enhanced by assuming ad hoc that the complexes are higher oligomers, such as $C_{nq}P_{np}$. This picture yields an even stronger cooperativity of complex formation using the same immiscibility parameters. Fig. 8 illustrates the effect of this assumption on the complex concentration profile. It will be seen that the transition region can be made arbitrarily sharp, going from complex in a phospholipid-rich liquid to complex in a cholesterol-rich liquid. The calculated average molecular area versus composition for this condensed oligomeric complex model (shown in Fig. 9) exhibits sharp features that are similar to the experimental results in Fig. 2. This version of the mean field thermodynamic model includes the superlattice model if it is assumed that the multimeric complexes $C_{nq}P_{np}$ have ordered structures of the types proposed previously (Virtanen et al., 1995; Tang et al., 1995). In line with the above discussion, this oligomerized product is written in terms of the reaction,

$$nqC + npP \leftrightarrow \langle C_{nq}P_{np} \rangle \tag{13}$$

An illustrative phase diagram with upper critical points is given in Fig. 10. It will be seen that the effect of the

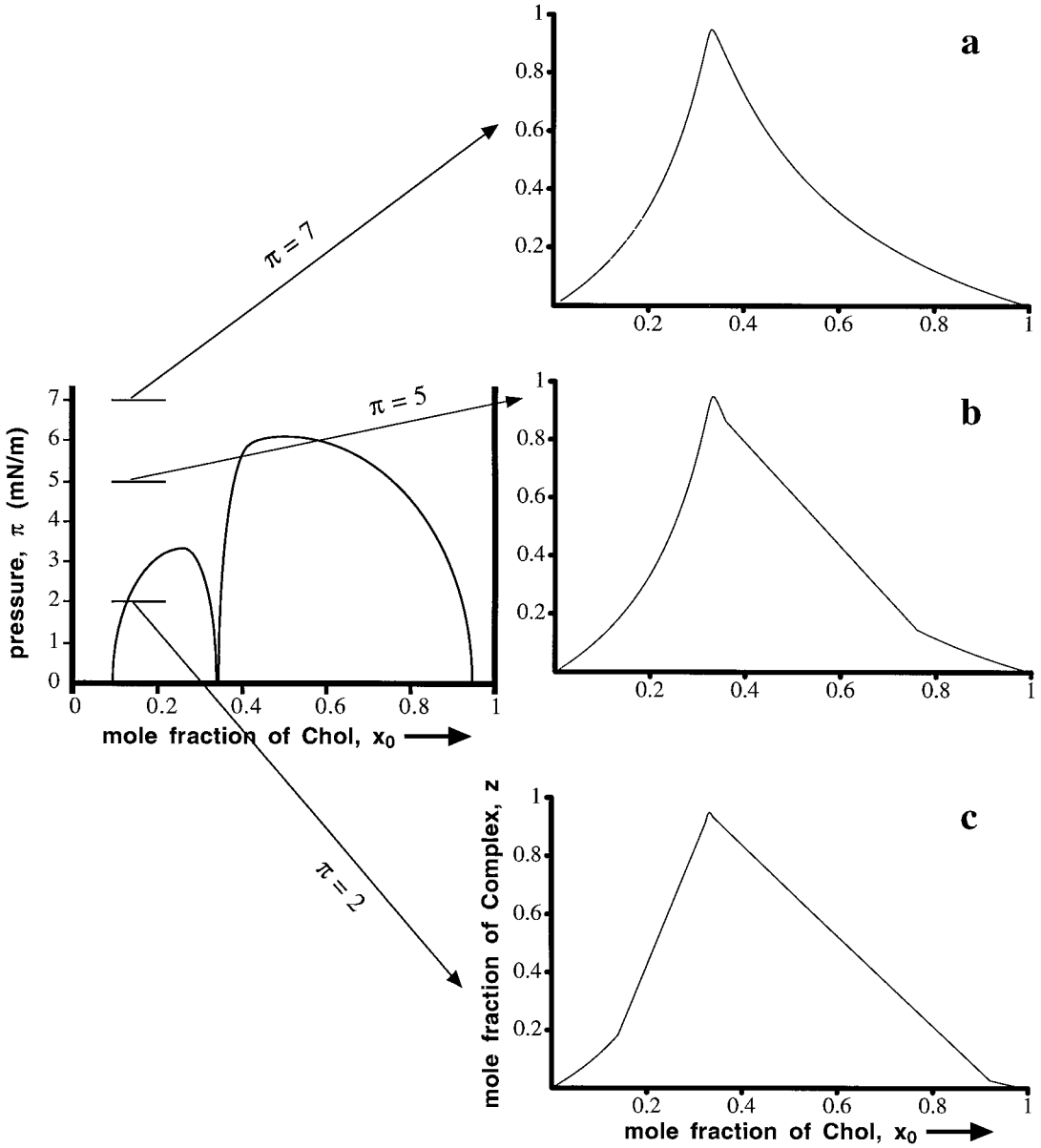

FIGURE 5 Complex concentration profiles as a function of the initial mole fraction of cholesterol (Chol), x_0, at various pressures for the system which yields the phase diagram of Fig. 4 *c*. The profiles are calculated for the most part using Eq. 9, except in the two-phase coexistence regions where the lever rule is invoked to obtain the amount of complex. (*a*) π = 7 mN/m; (*b*) π = 5 mN/m; (*c*) π = 2 mN/m.

oligomerization is to narrow the two-phase regions, and the region of the cusp.

There is a long history of proposals for complex stoichiometries in lipid monolayers and bilayers (Engelman and Rothman, 1972; Gershfeld, 1978; Albrecht et al., 1981; Presti et al., 1982; Müller-Landau and Cadenhead, 1979). Some of the earlier models have placed these molecules on lattice sites (Engelman and Rothman, 1972; Presti et al., 1982). More recently, several investigators have carried out studies of the fluorescence of various probes in phospholipid-cholesterol bilayer mixtures and have reported a number of kinks, maxima, and minima in fluorescence properties as a function of cholesterol concentration at putative stoichiometric compositions (Virtanen et al., 1995; Wang et al., 1998; Tang et al., 1995; Parassassi et al., 1995). These stoichiometries correspond, for example, to $q/p \cong 1/4, 2/7, 1/3, 1/2, 2/3, 1/1$. The various features have been attributed to the presence of superlattices. These superlattices are thought of as structures in which there are repulsions between cholesterol molecules (Wang et al., 1998; Somerharju et al., 1985; Sugar et al., 1994). (Some of this earlier work (Somerharju et al., 1985) dealt with the distribution of pyrene-labeled acyl chains of lipids, and the principle was subsequently applied to cholesterol distributions. Lateral ordering of lipids in DMPC-cardiolipin mixtures has also been proposed (Berclaz and McConnell, 1981)). As a con-

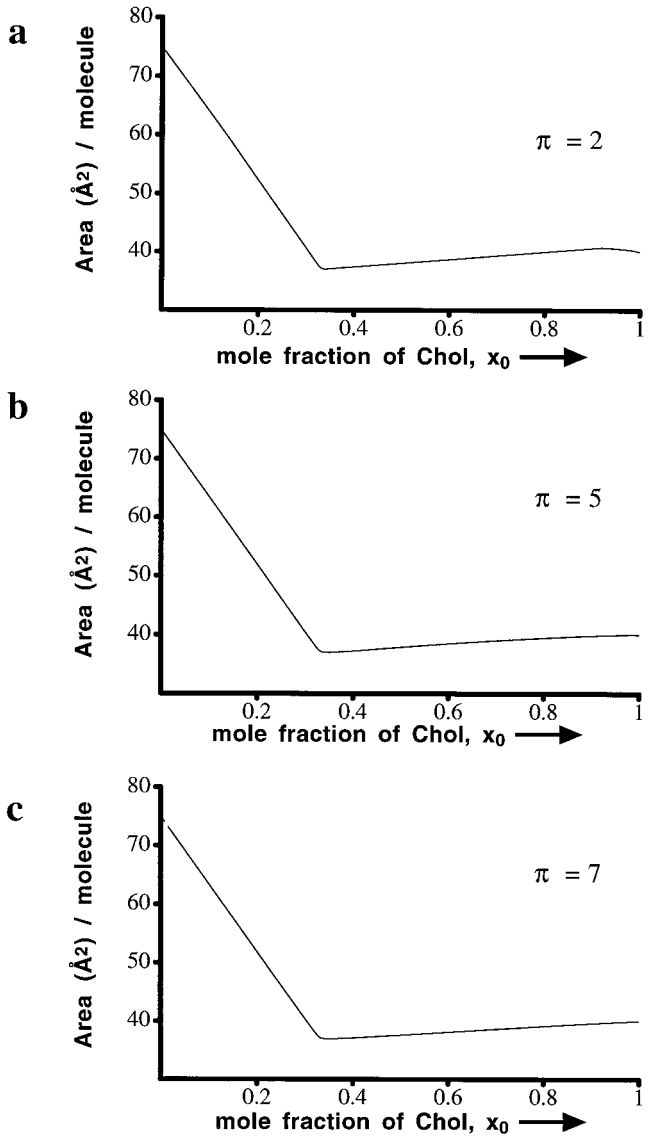

FIGURE 6 Calculations of average molecular areas as a function of the initial mole fraction of cholesterol (Chol), x_0, at various pressures for the system yielding the phase diagram of Fig. 4 *c*. The average molecular area is obtained by differentiating Eq. 3, the free energy function, with respect to π. Equation 9 gives the mole fractions of each of the components. In these calculations, $A_x^0 = 40$ Å^2/molecule, $A_y^0 = 75$ Å^2/molecule, and all other values are the same as for Fig. 4 *c*. (*a*) $\pi = 2$ mN/m; (*b*) $\pi = 5$ mN/m; (*c*) $\pi = 7$ mN/m.

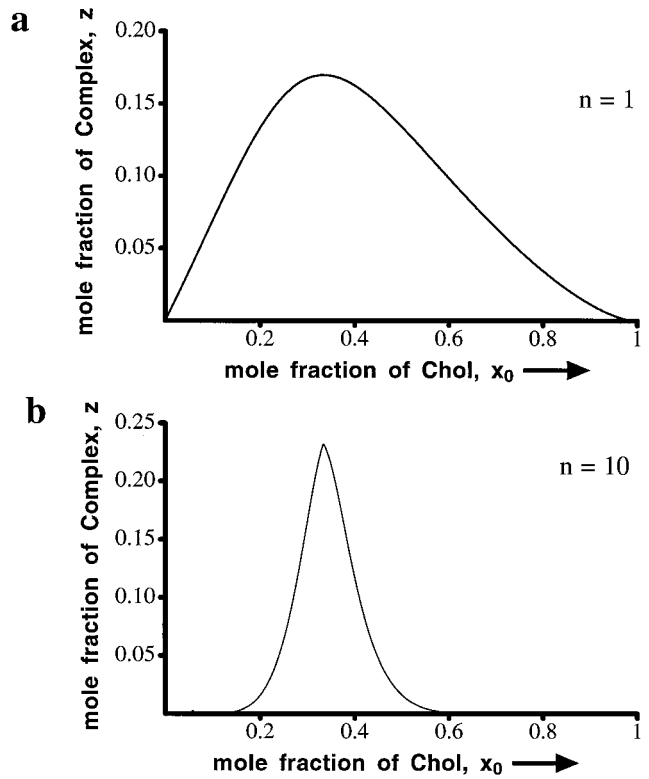

FIGURE 7 Complex concentration profiles as a function of the initial mole fraction of cholesterol (Chol), x_0, for an ideal reaction $nqC + npP \leftrightarrow C_{nq}P_{np}$ with equilibrium constant $K = 2$. (*a*) Degree of complex formation when $n = 1$, $q = 1$, $p = 2$. (*b*) Degree of complex formation when $n = 10$, $q = 1$, $p = 2$.

sequence, cholesterol molecules are imagined to be positioned remotely from one another on presumed lattice sites. The experimental results obtained by these more recent investigators are generally compatible with the thermodynamic model presented here in the sense that the model predicts sharp changes in certain membrane properties as composition is changed. For example, in passing from one two-phase region to another, the interdomain line tension is expected to change abruptly. Probes that partition at the interface between domains should then show significant changes in properties at these compositions. Probes that do *not* partition into the condensed complex phase would also undergo an abrupt change of environment when composition is changed so as to pass from the α two-phase region to the β two-phase region. Even in the homogeneous phase strong variations in complex, phospholipid, and free cholesterol concentrations such as those illustrated in Figs. 5 and 8 might give rise to the observed changes in fluorescence properties, particularly those measurements that depend on partitioning of the probe into the membrane. In some experiments, these rather abrupt changes in composition might easily be mistaken for a liquid-liquid phase boundary. Experimentally we cannot rule out the possibility that multiple complexes are formed in the monolayers, and only some are revealed by the upper miscibility critical points. In some respects a *theoretical superlattice model* that invokes cholesterol-cholesterol repulsions might not appear consistent with our experimental results and the corresponding thermodynamic model. For example in the α liquid-liquid two phase regions, the cholesterol molecules do not stay as far apart as possible, but rather concentrate in the condensed complex liquid phase, and above the critical pressures the complexes are completely miscible with the other components. However, above the critical pressures, the thermodynamic model can give results very suggestive of the data used in support of the superlattice model. It will be seen in Fig. 8 *e* that almost spikelike variations in

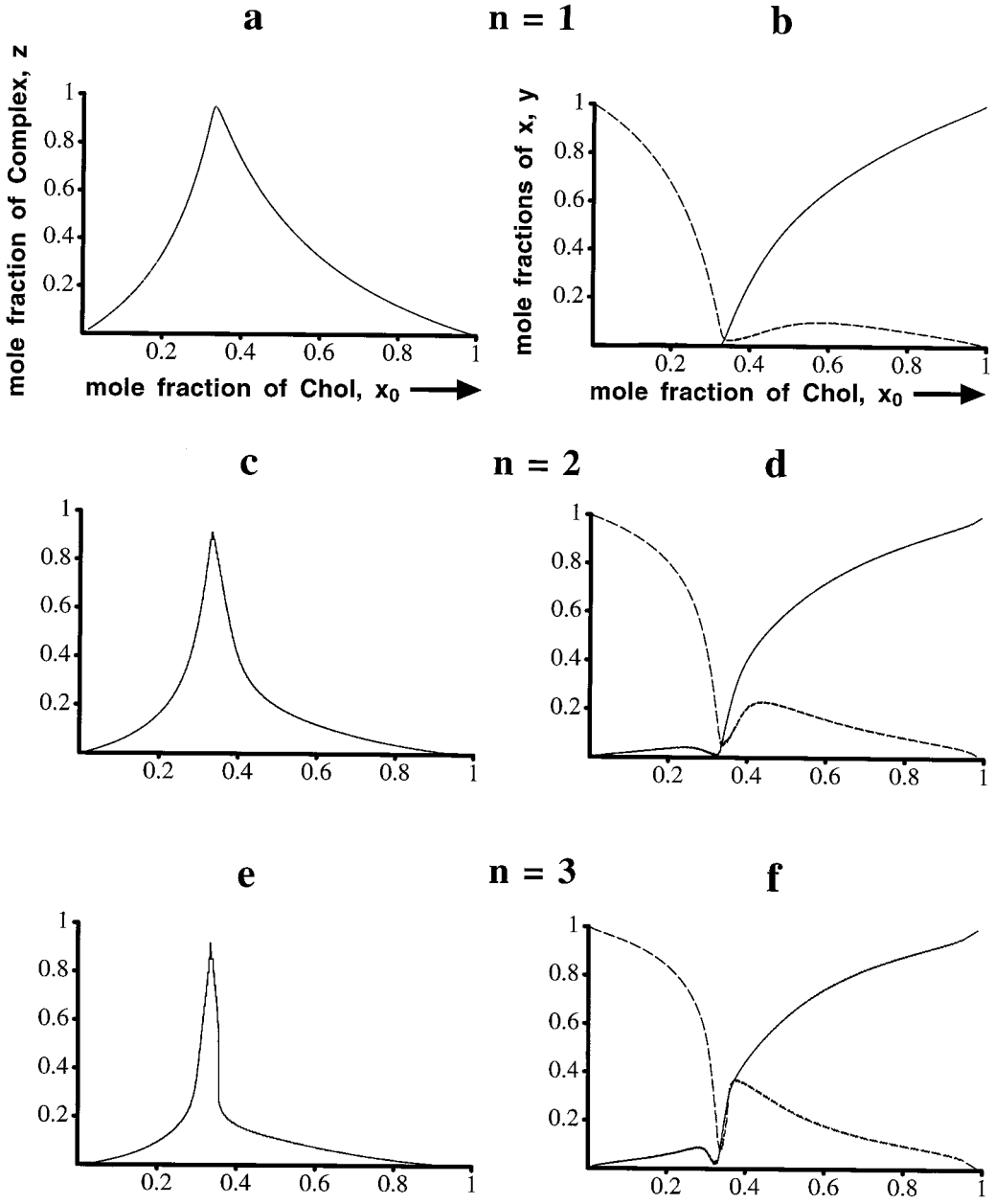

FIGURE 8 Concentrations of cholesterol, phospholipids, and complex as a function of the initial mole fraction of cholesterol (Chol), x_0, for the system with the same parameters as for Fig. 4 *c*. This calculation considers multimeric complexes, $\langle C_{nq}P_{np}\rangle$, where the stoichiometries in Eq. 1 are nq and np, instead of q and p. The profiles are calculated for the one-phase region at a pressure of 7 mN/m. The effect of increasing n is seen as one goes from (*a*) and (*b*) to (*c*) and (*d*) and finally to (*e*) and (*f*). In (*b*), (*d*), and (*f*) the dashed line represents the mole fraction of phospholipid, y, and the solid line represents the mole fraction of cholesterol, x. (*a*) Degree of complex formation when $n = 1$. (*b*) Cholesterol and phospholipid mole fractions when $n = 1$. (*c*) Degree of complex formation when $n = 2$. (*d*) Cholesterol and phospholipid mole fractions when $n = 2$. (*e*) Degree of complex formation when $n = 3$. (*f*) Cholesterol and phospholipid mole fractions when $n = 3$.

condensed complex concentration can be achieved with even modest oligomerization. One need only assume the formation of a number of such complexes with different stoichiometries so as to achieve a series of spikelike condensed complex concentration profiles, which could easily mimic the reported data from fluorescence probes, and observations on phospholipase action (Liu and Chong, 1999).

The calculations used here employ a mean field model to describe several intermolecular interactions. Corrales and Wheeler have obtained substantially similar phase diagrams using a decorated lattice model with nearest-neighbor interactions, so the mean-field approximation in itself is not required to produce immiscibilities (Corrales and Wheeler, 1989). Nearest-neighbor anisotropic intermolecular forces have also been used to calculate pairs of upper miscibility

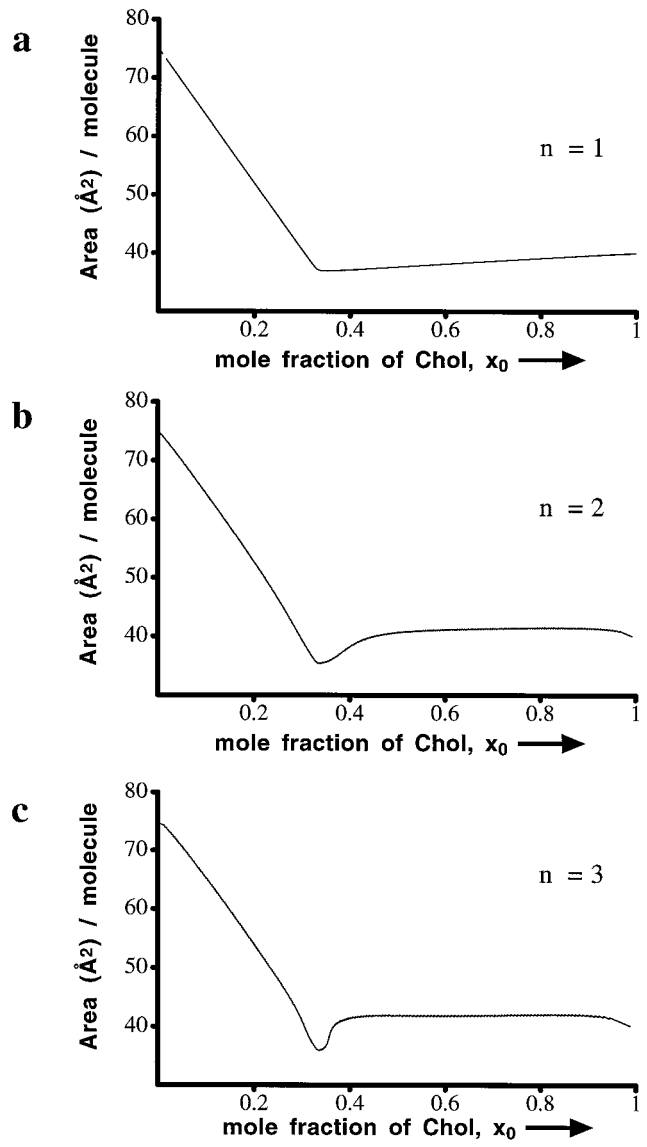

FIGURE 9 Calculations of average molecular areas as a function of the initial mole fraction of cholesterol (Chol), x_0, for the systems in Fig. 8 that take into account the formation of multimeric complexes, $\langle C_{nq}P_{np}\rangle$. The areas are calculated for the one phase region at a pressure of 7 mN/m. The average molecular area is obtained by differentiating Eq. 3, the free energy function, with respect to π. Equation 9 yields the mole fractions of each of the components. Values of 40 and 75 Å^2/molecule are used for A_x^0 and A_y^0, respectively. Other values used are the same as for Fig. 4 *c*. (*a*) $n = 1$ *and* $\Delta A = -40$ Å^2; mole fractions of the three components are shown in Fig. 8, *a* and *b*. (*b*) $n = 2$ and $\Delta A = -120$ Å^2; mole fractions of the three components are shown in Fig. 8, *c* and *d*. (*c*) $n = 3$ and $\Delta A = -240$ Å^2; mole fractions of the three components are shown in Fig. 8, *e* and *f*.

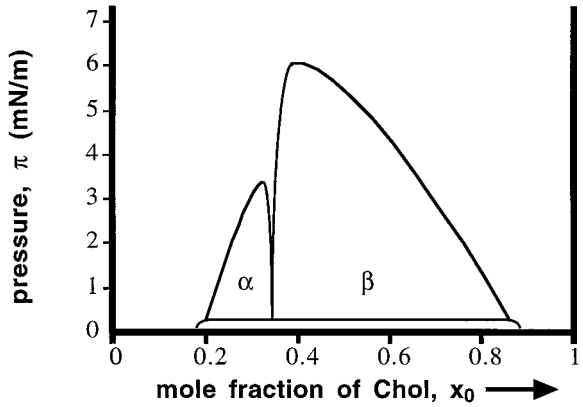

FIGURE 10 Calculated phase diagram for a binary reaction mixture of cholesterol and phospholipids with the same parameters as the phase diagram in Fig. 4 *c,* except that this calculation considers multimeric complexes where the stoichiometries in Eq. 1 are *nq* and *np*, instead of *q* and *p*. For this particular phase diagram, $n = 3$.

critical points, but the calculated phase diagrams are distinctly different from those reported here (Hueda et al., 1997). Huang and Feigenson (1999) have recently used Monte Carlo simulations with multibody interactions to simulate phospholipid-cholesterol mixtures. It is possible that such lattice-based calculations may also yield pairs of upper miscibility critical points. However, such multibody interactions may simulate complex formation. An interesting point relevant to the mean field picture concerns the use of the "average phospholipid" in the model calculations for mixtures of phospholipids. This approximation implies that the phase diagram curves are binodal curves, which in turn implies that the critical points must be at the peaks of these curves. In all experiments thus far this has been found to be the case.

As noted in the Introduction, the observation of two upper miscibility critical points in monolayer membranes has led us to apply this thermodynamic model to cholesterol-phospholipid mixtures. The model is quite general, and appears to be consistent with many earlier experimental observations and some, but possibly not all, aspects of earlier theoretical models. The model is strongly supported by the measurements of average molecular area versus composition that show sharp features at the stoichiometric compositions. When this mean-field thermodynamic model is extrapolated to lipid bilayers and biological membranes, it is reasonable to conclude that *condensed complexes* are responsible for the "condensing effect" of cholesterol and the "liquid condensed phase." It is also plausible that the condensed complexes are involved in "detergent-resistant membrane rafts" isolated from biological membranes (Xavier et al., 1998; Viola et al., 1999; Sheets et al., 1999; Brown and Rose, 1992; Brown and London, 1998; Simons and Ikonen, 1997). Even though the quantitative correspondence between physical chemical properties of lipid monolayers and bilayers is not complete, a number of these properties are sufficiently similar that these extrapolations appear to be safe.

The ease with which pressure changes can be made in monolayers provides a convenient means for dissecting selective intermolecular forces. At the lower pressures, molecules and groups of molecules tend to separate, except for the most stable groupings. The various immiscibilities found at lower pressures disappear at the higher pressures, but the thermodynamic model predicts that these complexes

remain at the higher pressures in the absence of phase separations. Irrespective of whether there are or are not liquid-liquid immiscibilities in cholesterol-phospholipid bilayers, the model leads to the expectation of reciprocal changes in the concentration of free phospholipid, and free cholesterol, on passing through the stoichiometric composition (Fig. 8). There is an even steeper increase in the cholesterol chemical *activity* on increasing cholesterol concentration above the stoichiometric composition (*activity* = $e^{\mu/kT}$). Thus, for example, the partition of cholesterol from the membrane into water should change significantly at this point. In cell membranes, this abrupt change in membrane free cholesterol activity might serve as a signal for total cholesterol concentration regulation by means of a membrane-bound "cholesterol sensor" that forms a transcription factor in cholesterol biosynthesis (Brown and Goldstein, 1999).

We thank Tom Anderson for help with Mathematica programming, Sarah Keller for invaluable help and advice throughout the course of these studies, and Michael Brown for a preprint of Brown and Goldstein (1999).

This work was supported by the National Science Foundation.

REFERENCES

Albrecht, O., H. Gruler, and E. Sackmann. 1981. Pressure-composition phase diagrams of cholesterol-lecithin, cholesterol/phosphatidic acid, and lecithin/phosphatidic acid monolayers: a Langmuir film balance study. *J. Colloid Interface Sci.* 79:319–338.

Benvegnu, D. J., and H. M. McConnell. 1993. Surface dipole densities in lipid monolayers. *J. Phys. Chem.* 97:6686–6691.

Berclaz, T., and H. M. McConnell. 1981. Phase equilibria in binary mixtures of dimyristoylphosphatidyl-choline and cardiolipin. *Biochemistry.* 20:6635–6640.

Bohuslav, J., T. Cinek, and V. Horejsi. 1993. Large, detergent resistant complexes containing murine antigens Thy-1 and Ly-6 and protein tyrosine kinase p56lck. *Eur. J. Immunol.* 23:825–831.

Brown, D. A., and E. London. 1998. Functions of lipid rafts in biological membranes. *Annu. Rev. Cell & Dev. Biol.* 14:111–136.

Brown, D. A., and J. K. Rose. 1992. Sorting of GPI-anchored proteins to glycolipid-enriched membrane subdomains during transport to the apical cell surface. *Cell.* 68:533–544.

Brown, M. S., and J. L. Goldstein. 1999. A proteolytic pathway that controls the cholesterol content of membranes, cells, and blood. *Proc. Natl. Acad. Sci. USA.* (in press).

Cinek, T., and V. Horejsi. 1992. The nature of large noncovalent complexes containing glycosyl-phosphatidylinositol-anchored membrane glycoproteins and protein tyrosine kinases. *J. Immunol.* 149:2262–2270.

Corrales, L. R., and J. C. Wheeler. 1989. Chemical reaction driven phase transitions and critical points. *J. Chem. Phys.* 91:7097–7112.

Engelman, D. M., and J. E. Rothman. 1972. The planar organization of lecithin-cholesterol bilayers. *J. Biol Chem.* 247:3694–3697.

Feingold, L. 1993. Cholesterol in membrane models. CRC Press, Ann Arbor, MI.

Gershfled, N. L. 1978. Equilibrium studies of lecithin-cholesterol interactions. I. *Biophys. J.* 22:469–488.

Hagen, J. P., and H. M. McConnell. 1996. Critical pressures in multicomponent lipid monolayers. *Biochim. Biophys. Acta.* 1280:169–172.

Hagen, J. P., and H. M. McConnell. 1997. Liquid-liquid immiscibility in lipid monolayers. *Biochim. Biophys. Acta.* 1329:7–11.

Hanada, K., M. Nishijama, Y. Akamatsu, and R. E. Pagano. 1995. Both sphingolipids and cholesterol participate in the detergent insolubility of alkaline phosphatase, a glycophosphatidylinositol-anchored protein, in mammalian membranes. *J. Biol. Chem.* 270:6254–6260.

Hirshfeld, C. L., and M. Seul. 1990. Critical mixing in monomolecular films: pressure-composition phase diagram of a two-dimensional binary mixture. *J. Phys. France.* 51:1537–1552.

Huang, J., and G. W. Feigenson. 1999. A microscopic interaction model of maximum solubility of cholesterol in lipid bilayers. *Biophys. J.* 76: 2142–2157.

Hueda, Y., M. E. Costas, and R. L. Scott. 1997. Quasi-chemical phase diagrams for orienting mixtures. *J. Phys. Chem. B.* 101:8676–8682.

Ipsen, J. H., G. Karlstrom, O. G. Mouritsen, H. Wennerstrom, and M. J. Zuckermann. 1987. Phase equilibria in the phosphatidylcholine-cholesterol system. *Biochim. Biophys. Acta.* 905:162–172.

Keller, S. L., and H. M. McConnell. 1999. Stripe phases in lipid monolayers near a miscibility critical point. *Phys. Rev. Lett.* 82:1602–1605.

Lee, K. Y. C., J. F. Klingler, and H. M. McConnell. 1994. Electric field-induced concentration gradients in lipid monolayers. *Science.* 263: 655–658.

Liu, F., and P. L. Chong. 1999. Evidence for a regulatory role of cholesterol superlattices in the hydrolytic activity of secretory phospholipase A2 in lipid membranes. *Biochemistry.* 38:3867–3873.

Müller-Landau, F., and D. A. Cadenhead. 1979. Molecular packing in steroid-lecithin monolayers. 2. Mixed films of cholesterol with dipalmitoylphosphatidylcholine and tetradecanoic acid. *Chem. Phys. Lipids.* 25:315–328.

Parassassi, T., A. M. Giusti, M. Raimondi, and E. Gratton. 1995. Abrupt modifications of phospholipid bilayer properties at critical cholesterol concentrations. *Biophys. J.* 68:1895–1902.

Presti, F. T., R. J. Pace, and S. I. Chan. 1982. Cholesterol-phospholipid interaction in membranes. 2. Stoichiometry and molecular packing of cholesterol-rich domains. *Biochemistry.* 21:3831–3835.

Radhakrishnan, A., and H. M. McConnell. 1999. Cholesterol-phospholipid complexes in membranes. *J. Am. Chem. Soc.* 121:486–487.

Sheets, E. D., D. Holowka, and B. Baird. 1999. Membrane organization in immunoglobulin E receptor signaling. *Curr. Opin. Chem. Biol.* 3:95–99.

Simons, K., and E. Ikonen. 1997. Functional rafts in cell membranes. *Nature.* 387:569–572.

Slater, G., and A. Caille. 1981. A new theoretical approach to study the effects of active molecules on lipid bilayer properties: the cholesterol problem. *Phys. Lett. A.* 86:256–258.

Somerharju, P., J. A. Virtanen, K. K. Eklund, P. Vainio, and P. K. J. Kinnunen. 1985. 1-palmitoyl-2-pyrenedecanoyl glycerophospholipids as membrane probes: evidence for regular distribution in liquid-crystalline phosphatidylcholine bilayers. *Biochemistry.* 24:2773–2781.

Subramaniam, S., and H. M. McConnell. 1987. Critical mixing in monolayer mixtures of phospholipid and cholesterol. *J. Phys. Chem.* 91: 1715–1718.

Sugar, I. P., D. Tang, and P. L. Chong. 1994. Monte Carlo simulation of lateral distribution of molecules in a two-component lipid membrane. Effect of long-range repulsive interactions. *J. Phys. Chem.* 98: 7201–7210.

Talanquer, V. 1992. Global phase diagram for reacting systems. *J. Chem. Phys.* 96:5408–5421.

Tang, D., W. van Der Meer, and S.-Y. S. Cheng. 1995. Evidence for a regular distribution of cholesterol in phospholipid bilayers from diphenylhexatriene fluorescence. *Biophys. J.* 68:1944–1951.

Viola, A., S. Schroeder, Y. Sakakibara, and A. Lanzavecchia. 1999. T lymphocyte costimulation mediated by reorganization of membrane microdomains. *Science.* 283:680–682.

Virtanen, J. A., M. Ruonala, M. Vauhkonen, and P. Somerharju. 1995. Lateral organization of liquid-crystalline cholesterol-dimyristoylphosphatidylcholine bilayers. Evidence for domains with hexagonal and centered rectangular cholesterol superlattices. *Biochemistry.* 34: 11568–11581.

Wang, M. M., I. P. Sugar, and P. L. Chong. 1998. Role of the sterol superlattice in the partitioning of the antifungal drug nystatin into lipid membranes. *Biochemistry.* 37:11797–11805.

Xavier, R., T. Brennan, Q. Q. Li, C. McCormack, and B. Seed. 1998. Membrane compartmentation is required for efficient T-cell activation. *Immunity.* 8:723–732.